ANNALS OF FACULTY ENGINEERING HUNEDOARA
- INTERNATIONAL JOURNAL OF ENGINEERING
Tome IX (Year 2011). Fascicule 1. (ISSN 1584 - 2665)

[1.] Paolo BOSCARIOL

EXPERIMENTAL VALIDATION OF A SPECIAL STATE OBSERVER FOR A CLASS OF FLEXIBLE LINK MECHANISMS

[1.] UNIVERSITY OF UDINE – DIEGM, Udine, ITALY

ABSTRACT: This paper presents an experimental validation of a state observer for flexible-link manipulators (FLM). The design of this observer is based on an accurate dynamic model of the mechanisms, able to take into account the coupled rigid-flexible dynamics of the system. Experimental results on a single-link manipulator affected by gravity force show that the proposed observer achieves a good estimation of the plant dynamics even if the displacement signal is not measured. The evaluation of the performance is done experimentally by comparing the estimated elastic displacement with the measures obtained on the field.
KEYWORDS: flexible-link manipulators (FLM), mechanisms, dynamic model

❖ INTRODUCTION

Dynamics and control of flexible-link mechanisms are topics of a widespread interest in the scientific literature. From the 70's, a large number of papers have been published: Dwivedy [1] cites 433 works from 1975 to 2005 on the modeling of this class of mechanism and Benosman [2] cites 119 papers up to 2003. This popularity is motivated by several advantages of flexible-link manipulators over their rigid counterpart, such as lower weight, higher operative speed and reduced power consumption. Nevertheless, specific solutions in terms of control must be used to reach satisfactory performance, high accuracy and stability.

Model-based control strategy for flexible manipulators, such as [3,4,5] by the same Author or [6] and [7], just to mention some recent works, requires the use of state observers to estimate the evolution of the dynamics of the plant. The estimation of the dynamics of such plant is essential, since complexity of the motion would otherwise require the use of a very large number of sensors. In this case the proposed state-space observer requires the measure of only the angular position of the mechanism and the instant value of the torque applied to the mechanism, so it does not require the use of other sensor such as strain gauge bridges or accelerometers. For example in [8] a strain gauge bridge is adopted to measure the elastic deformation of a four links FLM.

The test bench is a single-link flexible mechanism affected by gravity force. The performance of the proposed Kalman state observer is evaluated experimentally. The estimation of the state of the plant is based only on the measure of the angular position of the hub and on the torque signal, thus reducing the effects of measures such as strain gauge signal which are usually affected by noise. The accuracy of such system is evaluated experimentally by comparing the estimated state with the measure of the elastic displacements performed by a strain gauge transducer.

❖ THE STUDY

In this section the dynamic model of a flexible-link mechanism suggested by Giovagnoni [9] will be briefly explained. The choice of this formulation among the several proposed in the last 30 years has been motivated by the high grade of accuracy provided by this model, which has been proved several times, for example in [10,11]. The main characteristics of this model can be summarized in four points:

1. finite element (FEM) formulation
2. Equivalent Rigid-Link System (ERLS) formulation [12]
3. mutual dependence of the rigid and flexible motion
4. capability of describing mechanisms with an arbitrary number of flexible and rigid links

First, each flexible link of the mechanism is subdivided into several finite elements. Referring to the Figure 1 the following vectors, calculated in the global reference frame {X,Y, Z}, can be defined:

- $\boldsymbol{r}_i$ and $\boldsymbol{u}_i$ are the vectors of nodal position and nodal displacement in the i-th element of the ERLS
- $\boldsymbol{p}_i$ is the position of a generic point inside the i-th element
- $\boldsymbol{q}$ is the vector of generalized coordinates of the ERLS

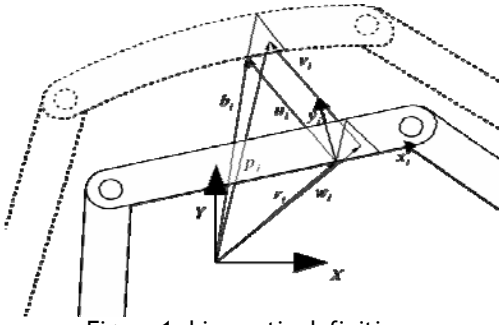

Figure 1: kinematic definitions

The vectors defined so far are calculated in the global reference frame {X,Y,Z}. Applying the principle of virtual work:

$$\delta W^{elastic} + \delta W^{external} + \delta W^{inertia} = 0$$

the following relation can be stated:

$$\sum_i \int_{V_i} \delta \mathbf{p}_i^T \ddot{\mathbf{p}}_i \rho_i dw + \sum_i \int_{V_i} \delta \check{\eta}_i^T \mathbf{D}_i \check{\eta}_i dw = \sum_i \int_{V_i} \delta \mathbf{p}_i^T \mathbf{g} \rho dw + (\delta \mathbf{u}^T + \delta \mathbf{r}^T)\mathbf{F} \tag{1}$$

ε_i, $\boldsymbol{D}_i$, ρ_i and $\delta\varepsilon_i$ are the strain vector, the stress-strain matrix, the mass density of the i-th link and the virtual strains, respectively. $\boldsymbol{F}$ is the vector of the external forces, including the gravity, whose acceleration vector is g. Eq. 1 shows the virtual works of inertial, elastic and external forces, respectively.

From this equation, $\delta \boldsymbol{p}_i$ and $\ddot{\boldsymbol{p}}_i$ for a generic point in the i-th element are:

$$\delta \mathbf{p}_i = \mathbf{R}_i \mathbf{N}_i \mathbf{T}_i \delta \mathbf{r}_i$$
$$\ddot{\mathbf{p}}_i = \mathbf{R}_i \mathbf{N}_i \mathbf{T}_i + 2(\dot{\mathbf{R}}_i \mathbf{N}_i \mathbf{T}_i + \mathbf{R}_i \mathbf{N}_i \dot{\mathbf{T}}_i)\dot{\mathbf{u}}_i \tag{2}$$

where $\boldsymbol{T}_i$ is a matrix that describes the transformation from global-to local reference frame of the i-th element, $\boldsymbol{R}_i$ is the local-to-global rotation matrix and $\boldsymbol{N}_i$ is the shape function matrix. Taking $\mathbf{B}_i(x_i, y_i, z_i)$ as the strain-displacement matrix, the following relation holds:

$$\check{\eta}_i = \mathbf{B}_i \mathbf{T}_i \delta \mathbf{u}_i$$
$$\delta \check{\eta}_i = \mathbf{B}_i \delta \mathbf{T}_i \mathbf{u}_i + \mathbf{B}_i \mathbf{T}_i \delta \mathbf{u}_i \tag{3}$$

Since nodal elastic virtual displacements ($\partial \boldsymbol{u}$) and nodal virtual displacements of the ERLS ($\partial \boldsymbol{r}$) are independent from each other, from the relations reported above the resulting equation describing the motion of the system is:

$$\begin{bmatrix} \mathbf{M} & \mathbf{MS} \\ \mathbf{S}^T\mathbf{M} & \mathbf{S}^T\mathbf{MS} \end{bmatrix} \begin{bmatrix} \ddot{\mathbf{u}} \\ \ddot{\mathbf{q}} \end{bmatrix} = \begin{bmatrix} \mathbf{f} \\ \mathbf{S}^T\mathbf{f} \end{bmatrix} \tag{4}$$

$\boldsymbol{M}$ is the mass matrix of the whole system and $\boldsymbol{S}$ is the sensitivity matrix for all the nodes. Vector $\mathbf{f} = \mathbf{f}(\mathbf{u}, \dot{\mathbf{u}}, \mathbf{q}, \dot{\mathbf{q}})$ accounts for all the forces affecting the system, including the gravity force. Adding a Rayleigh damping, the right-hand side of Eq. 4 becomes:

$$\begin{bmatrix} \mathbf{f} \\ \mathbf{S}^T\mathbf{f} \end{bmatrix} = \begin{bmatrix} -2\mathbf{M}_G - \alpha\mathbf{M} - \beta\mathbf{K} & -\mathbf{M}\dot{\mathbf{S}} & -\mathbf{K} \\ \mathbf{S}^T(-2\mathbf{M}_G - \alpha\mathbf{M}) & -\mathbf{S}^T\mathbf{M}\dot{\mathbf{S}} & 0 \end{bmatrix} \begin{bmatrix} \dot{\mathbf{u}} \\ \dot{\mathbf{q}} \\ \mathbf{u} \end{bmatrix} + \begin{bmatrix} \mathbf{M} & \mathbf{I} \\ \mathbf{S}^T\mathbf{M} & \mathbf{S}^T \end{bmatrix} \begin{bmatrix} \mathbf{g} \\ \mathbf{F} \end{bmatrix} \tag{5}$$

Matrix $\boldsymbol{MG}$ accounts for the Coriolis contribution, while $\boldsymbol{K}$ is the stiffness matrix of the whole system. α and β are the two Rayleigh damping coefficients. System in (4) and (5) can be made solvable by forcing to zero as many elastic displacement as the generalized coordinates, in this way ERLS position is defined univocally. Therefore removing the displacement forced to zero from (4) and (5) gives:

$$\begin{bmatrix} \mathbf{M}_{in} & (\mathbf{MS})_{in} \\ (\mathbf{S}^T\mathbf{M})_{in} & \mathbf{S}^T\mathbf{MS} \end{bmatrix} \begin{bmatrix} \ddot{\mathbf{u}}_{in} \\ \ddot{\mathbf{q}} \end{bmatrix} = \begin{bmatrix} \mathbf{f}_{in} \\ \mathbf{S}^T\mathbf{f} \end{bmatrix} \tag{6}$$

The values of the accelerations can be computed at each step by solving the system in (6), while the values of velocities and displacements can be obtained by an appropriate integration scheme (e.g. the Runge-Kutta algorithm). It is important to focus the attention on the size and the rank of the matrices involved in (6), and also to the choice of the general coordinates used in the ERLS definition. Otherwise it might happen that a singular configuration is encountered during the motion of the mechanism [9]. In this case, (6) cannot be solved.

❖ ANALISES, DISCUSIONS, APPROACHES AND INTERPRETATIONS. EXPERIMENTAL SETUP

In the first part of this section the experimental setup and the test bench single-link flexible manipulator are briefly described. Then the equations and the design of the proposed state observer are introduced. In the last part of the section the experimental results of the observer used with a PID position control are shown and discussed.

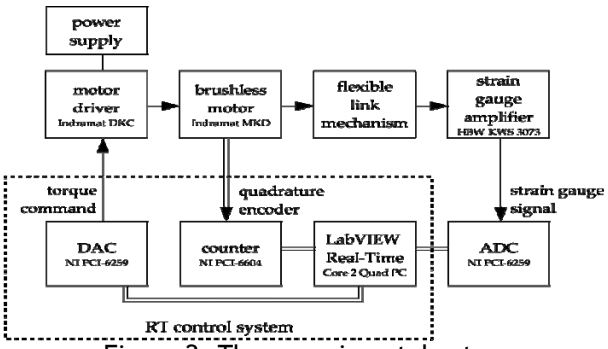

Figure 2: The experimental setup

Table 1: structural and dynamic characteristics of the flexible rod

	Symbol	Value
Young's modulus	E	230 × 109 [Pa]
Flexural stiffness	EJ	191.67 [Nm4]
Beam width	a	1 × 10−2 [m]
Beam thickness	b	1 × 10−2 [m]
Mass/unit length	m	0.7880 [kg/m]
Flexible Link length	l	1.5 [m]
Strain sensor position	s	0.75 [m]
First Rayleigh damping constant	α	4.5 × 10−1 [s−1]
Second Rayleigh damping constant	β	4.2 × 10−5 [s−1]

Figure 3: The flexible-link mechanism used for experimental tests

The plant used to evaluate the effectiveness of the proposed predictive control strategy is a single-link flexible mechanism. It is made by a long and thin steel rod, actuated by a brushless motor. No reduction gears are used, so one end of the link is rigidly coupled to the motor shaft. The flexible link can rotate on the vertical plane, so the mechanism dynamics is heavily affected by the gravity force. The structural and dynamic characteristics of the flexible rod can be found in Table 1. Owing to the overall dimensions, the mechanism has a limited movement range (around ± 25 [deg]) from the vertical position. The motion of the link is governed trough an Indramat DKC-MKD brushless servo drive system. This drive is used as a torque generator, i.e. the instant value of the torque applied by the motor can be controlled by using an analog signal. Such a signal is supplied by a National Instruments PCI-6259 DAQ board, controlled by a Core 2 Quad PC.

The angular position is measured by a 4000 cpr quadrature encoder is read with a National Instruments PCI-6602 board. The strain gauge signal is measured with the same PCI-6259 board used to generate the torque reference signal, as it is visible in Figure 3. The data acquisition and the control software runs over the LabVIEW Real-Time OS.

The dynamic model can be described with a good accuracy it with four finite elements. This discretization is sufficient to describe accurately the first four modes of vibration: 23 Hz, 63 Hz, 124 Hz, 206 Hz. Higher order modes can be neglected as they have low energy and high damping values.

❖ DESIGN OF THE STATE OBSERVER

Most model-based control strategies can be applied only when a measure of the whole state $\boldsymbol{x}$ is available. In this application, there are only two measured values, so a state observer must be used. Here a Kalman asymptotic estimator has been chosen. An estimation of $\boldsymbol{x}(k)$ and $\boldsymbol{x}_m(k)$ (where $\boldsymbol{x}(k)$ is the state of the plant model and $\boldsymbol{x}_m(k)$ is the state of the measurement noise model) can be computed from the measured output $\boldsymbol{y}_m(k)$ as:

$$\begin{bmatrix} \hat{\mathbf{x}}(k \mid k) \\ \hat{\mathbf{x}}_m(k \mid k) \end{bmatrix} = \begin{bmatrix} \hat{\mathbf{x}}(k \mid k-1) \\ \hat{\mathbf{x}}_m(k \mid k-1) \end{bmatrix} + \mathbf{L}\left(\mathbf{y}_m(k) - \hat{\mathbf{y}}_m(k)\right) \tag{7}$$

$$\begin{bmatrix} \hat{\mathbf{x}}(k+1 \mid k) \\ \hat{\mathbf{x}}_m(k+1 \mid k) \end{bmatrix} = \begin{bmatrix} \mathbf{A}\,\hat{\mathbf{x}}(k \mid k) + \mathbf{B}\,\mathbf{z}(k) \\ \mathbf{A}\,\hat{\mathbf{x}}_m(k \mid k) \end{bmatrix}$$

$$\hat{\mathbf{y}}_m(k) = \mathbf{C}_m\,\hat{\mathbf{x}}(k \mid k-1)$$

The gain matrix $\boldsymbol{L}$ has been designed by using Kalman filtering techniques (see Franklin et al. [13]). The design of both the estimator and the prediction model is based on a linear state-space model of the FLM which has been obtained by applying the linearization procedure developed by Gasparetto in [14] to Eq. (6). The resulting state-space model can be rewritten as:

$$\begin{cases} \dot{\mathbf{x}}(t) = \mathbf{A}\mathbf{x}(t) + \mathbf{B}\mathbf{z}(t) \\ \mathbf{y}(t) = \mathbf{C}\mathbf{x}(t) \end{cases} \tag{8}$$

where $A \in R^{[26]} \times R^{[26]}$, $B \in R^{[26]} \times R^{[1]}$, $C \in R^{[2]} \times R^{[26]}$ are time-invariant matrices.

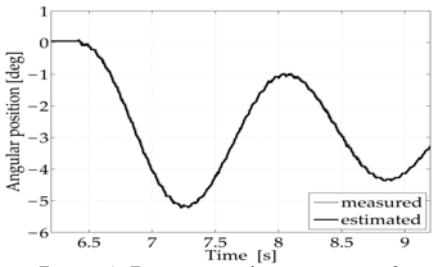

Figure 4: Experimental comparison of measured and estimated angular position

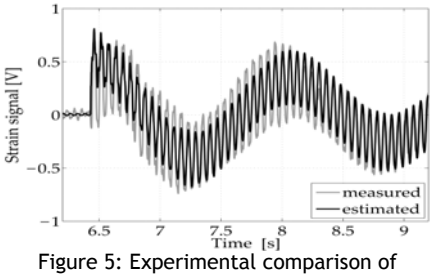

Figure 5: Experimental comparison of measured and estimated elastic displacement

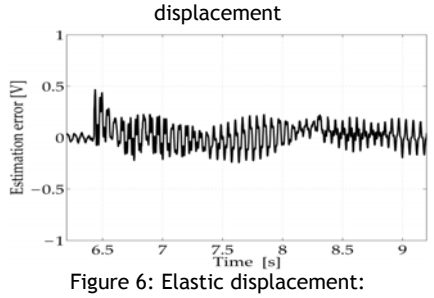

Figure 6: Elastic displacement: estimation error

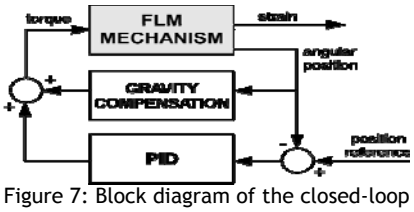

Figure 7: Block diagram of the closed-loop control system

The state vector $\boldsymbol{x}$ includes all the nodal displacements and the angular position q, as well as their time derivatives:

$$\mathbf{x}(t) = [u_1, u_2, \ldots, u_{13}, q, \dot{u}_i, \dot{u}_2, \ldots, \dot{u}_{13}, \dot{q}]^T \quad (9)$$

The output vector of the LTI system consists of two elements: $\mathbf{y}(t) = [u_6, q]^T$, being u_6 the rotational displacement at the midspan of the link. The input vector $\boldsymbol{z}(t)$ includes the torque applied to the link as single element. A comparison of measured and estimated values of the link curvature is reported in Figures 3,4,5. As it can be seen, the value of the elastic displacement can be evaluated with a good accuracy. The angular position of the mechanism is controlled with a PID controller with gravity compensation. The block diagram of the closed-loop control system is provided in Figure 6.

It must be pointed out that the state observer has the availability of only the quadrature encoder signal and the nominal torque applied to the rod. In this way, the robustness of the closed-loop system can be improved, since the measure of the strain gauge signal is heavily affected by noise. Moreover, the reduced number of sensor make this control strategy suitable to most robotic manipulators for industrial use, since sensors such as accelerometers and strain gauge bridges are usually unavailable on these systems.

❖ CONCLUSION

A state estimator for flexible-link mechanisms has been implemented and tested on a real single link mechanism. It has been proved experimentally that the state estimator used for all the experimental tests is capable of providing an accurate estimation of the plant dynamics with a very limited set of sensors. Such an estimator needs the measure of the angular position only and the torque applied by the brushless motor. For this reason, the proposed controller can be easily adapted to most of the industrial manipulators, which usually do not have sensors for measuring the elastic displacement of the links.

❖ REFERENCES

[1.] DWIVEDY, S., EBERHARD, P., 2006. Dynamic analysis of flexible manipulators, a literature review. Mechanism and Machine Theory 41 (7), 749–777. 17
[2.] BENOSMAN, M., LE VEY, G., 2004. Control of flexible manipulators: A survey. Robotica 22 (05), 533–545.
[3.] Boscariol, P., Gasparetto, A., Zanotto, V., 14-17 April 2009. Vibration reduction in a flexible link mechanism through the synthesis of an mpc controller. In: Proceedings of the 5th IEEE International Conference on Mechatronics (ICM2009). Malaga, Spain.
[4.] Boscariol, P., Gasparetto, A., Zanotto, V., January 2010. Active position and vibration control of a flexible links mechanism using model-based predictive control. Journal of Dynamic Systems, Measurement, and Control 132.
[5.] P. Boscariol, A. Gasparetto, V. Zanotto Model Predictive Control of a Flexible Links Mechanism Journal of Intelligent and Robotic Systems: Volume 58, Issue 2 (2010), Page 125-147
[6.] Hassan, M., Dubay, R., Li, C., Wang, R., 2007. Active vibration control of a flexible one-link manipulator using a multivariable predictive controller. Mechatronics 17 (6), 311–323.
[7.] Chalhoub, N., Kfoury, G., Bazzi, B., 2006. Design of robust controllers and a nonlinear observer for the control of a single-link flexible robotic manipulator. Journal of Sound and Vibration 291 (1-2), 437–461.
[8.] R. Caracciolo, A. Gasparetto, A. Trevisani and V. Zanotto. On the Design of State Observers for Flexible Link Mechanisms. In Proceedings of the 1st IASME International Conference on Advances in Mechanics and Mechatronics (483-144), Udine, Italy, March 2004
[9.] Giovagnoni, M., 1994. A numerical and experimental analysis of a chain of flexible bodies. Journal of Dynamic Systems, Measurement, and Control 116, 73–80.
[10.] Gasparetto, A., 2004. On the modeling of flexible-link planar mechanisms: experimental validation of an accurate dynamic model. Journal of dynamic systems, measurement, and control 126, 365.
[11.] Caracciolo, R., Richiedei, D., Trevisani, A., Zanotto, V., 2005. Robust mixed norm position and vibration control of flexible link mechanisms. Mechatronics 15 (7), 767–791.
[12.] Chang, L., Hamilton, J., 1991. The kinematics of robotic manipulators with flexible links using an equivalent rigid link system (ERLS) model. Journal of Dynamic Systems, Measurement, and Control 113, 48.
[13.] Franklin, G., Workman, M., Powell, D., 1997. Digital control of dynamic systems. Addison-Wesley Longman Publishing Co., Inc. Boston, MA, USA.
[14.] Gasparetto, A., 2001. Accurate modelling of a flexible-link planar mechanism by means of a linearized model in the state-space form for design of a vibration controller. Journal of Sound and vibration 240 (2), 241–262.